Path-Dependent Supercooling of the ³He Superfluid A-B transition*

Dmytro Lotnyk[1], Anna Eyal[1,2], Nikolay Zhelev[1], Abhilash Sebastian[1,3], Aldo
Chavez[1], Eric Smith[1], John Saunders[4], Erich Mueller[1] and Jeevak Parpia[1]

[1]*Department of Physics, Cornell University, Ithaca, NY, 14853 USA*
[2]*Physics Department, Technion, Haifa, Israel*
[3]*VTT Technical Research Centre of Finland Ltd, Espoo, Finland and*
[4]*Department of Physics, Royal Holloway University of London, Egham, TW20 0EX, Surrey, UK*
(Dated: December 29, 2020)

We examine the discontinuous first-order superfluid ³He A to B transition in the vicinity of the polycritical point (2.273 mK and 21.22 bar). We find path-dependent transitions: cooling at fixed pressure yields a well defined transition line in the temperature-pressure plane, but this line can be reliably crossed by depressurizing at nearly constant temperature after transiting T_c at a higher pressure. This path dependence is not consistent with any of the standard B-phase nucleation mechanisms in the literature.

Superfluid ³He is a condensed matter system w[...]
complex order parameter. The superfluid state oc[...]
with the condensation of pairs into a state with finit[...]
gular momentum via a second order phase transitio[...]
a pressure dependent transition temperature T_c. [...]
sure dependent strong coupling favors the anisotrop[...]
phase at high pressures (above the polycritical poi[...]
2.273 mK and 21.22 bar), while the isotropic B p[...]
is the stable phase below the $T_{AB}(P)$ line[1], term[...]
ing at the polycritical pressure. The transition bet[...]
the A and B phases is first order and thus subje[...]
hysteresis. A phase supercooling occurs because any[...]
mation of a bubble of radius r of B phase (from the [...]
ent A phase) sets off the unusually large surface er[...]
($\propto r^2$)[2] against the small free energy gain ($\propto -r^3$)[3][...]
leading to to a critical radius ≈ 1 μm. At high pres-
sure the A phase supercools well below T_{AB} and can be
long lived[4]. The extreme purity and low temperatures
that limit thermal fluctuations together with the bar-
rier to nucleation lead to calculated lifetimes of the A
phase greater than the age of the Universe. As Leggett
as pointed out[5–7], the nucleation mechanism of the B
phase "remains a mystery" and its study represents a
unique opportunity to gain fundamental insights[8]. The
transition was the subject of extensive experimental[9–
15] and theoretical investigation[5–7, 16–19].

Supercooling should be less near T_c at pressures (P)
and temperatures (T) in the vicinity of the polycritical
point (in low magnetic fields) since the free energies of
the two phases are nearly equal. The influence of differ-
ent phases thought to exist near T_c in bulk[20], and under
confinement[21] some of which have been observed in dis-
ordered ³He[22–24] may also play a role. Thus, the free
energy landscape would be different from that explored
far from T_c, and we concentrated our experimental in-
vestigation to this region of P, T (Supplementary Figure
1).

Two mechanisms for nucleation of the B phase have ex-
perimental support. The "Baked-Alaska mechanism"[6]
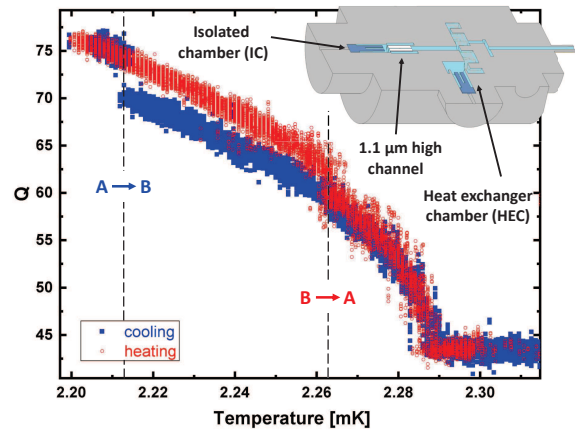requires local heating by deposition of energy following

FIG. 1. The quality factor Q of the quartz fork in the iso-
lated chamber while cooling (blue) and warming (red) at 21.8
bar with arrows marking the supercooled A→B and B→A
transitions. Inset shows a schematic of the experiment.

passage of a cosmic ray or charged particle and was tested
using quartz cells of roughness < 10 nm[13] and high
pressures far from T_c, where the free energy difference be-
tween the two phases is larger and lifetimes of the A phase
were long. The A→B transition in that experiment rarely
happened spontaneously, but could be induced by seed-
ing with a nearby radioactive source, confirming aspects
of the mechanism. In the cosmological or Kibble-Zurek
scenario[15–17], small regions undergo phase transitions
that are "oriented" differently under quench conditions
(cooling through T_c)[14, 15]. When they eventually coa-
lesce, they produce a cosmic string, or its equivalent in
³He - a vortex line. Other, yet to be tested models cite
Q balls[18] and Resonant Tunneling (RT)[19]. RT, in the
presence of adjacent energy states (or sub-phases) under
appropriate P, T conditions, enables the A→B transition.
It also makes the connection that RT should be present
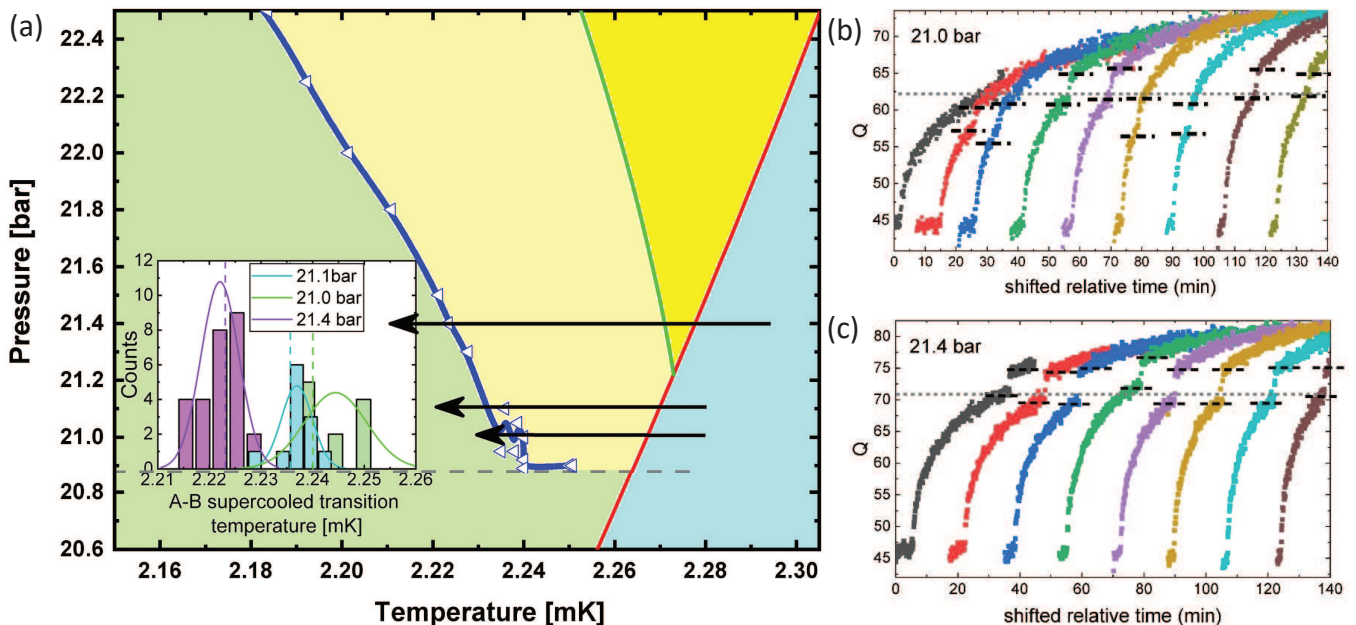in quantum field theory, the framework used to describe
³He properties[8, 19].

FIG. 2. (a) Blue, left-pointing triangles and the heavy blue line (guide to the eye) bound the supercooled A phase (light yellow). The red line marks the second-order phase transition $T_c(P)$, from the normal liquid to the superfluid state, the light green line $T_{AB}(P)$, separates the equilibrium A phase (dark yellow) from the B phase. The grey dashed line at 20.88 bar shows the limit of supercooled A phase observed under constant pressure cooling. A series of fast-cooled transitions (Q vs. time) are shown at 21.0 bar (b) and 21.4 bar (c) following heat pulses that carry the IC into the normal state. The Q of slow supercooled transitions (see Figure 1) are marked by dashed black lines. In (a) the arrows show trajectories of fast and slow cooled transitions including at 21.1 bar. In the inset to (a) we show the temperature distribution of fast-cooled transitions in relation to the slow-cooled transitions (dashed lines).

Our experiment consists of two chambers (Figure 1 inset, and Supplementary Figure 2) filled with bulk ^{3}He separated by a $D=1.1$ μm height channel.[25] Due to pairbreaking surface scattering, the B phase (with its uniform gap) is suppressed[26] relative to the A phase[27] whose point nodes align with surfaces, favoring the A phase at the temperatures and pressures discussed in this paper. Thus nucleation of the B phase in the chamber containing the silver sinter heat exchanger (HEC) (see Supplementary Figure 2) does not propogate into the isolated chamber (IC). There are no heterogeneous surfaces (e.g. sintered powders) in the IC to promote nucleation of the B phase but the surfaces are not specially prepared. The experiment is located where the magnetic field is ≤ 0.1 mT, the ^{3}He pressure, P was regulated to within ± 0.01 bar using a room temperature gauge (see Supplementary Note 1). Temperatures, T were read off from a ^{3}He melting curve thermometer[1] after correction for thermal gradients (≤ 15 μK[25]). During the experiment, we measure the resonant frequency, f, and the Q (Quality factor, $Q=f/\Delta f$ where Δf is the full linewidth at half power) of a quartz "fork"[28] immersed in bulk ^{3}He in the IC cooled by the heat exchanger through the channel[25]. The measured Q of the fork while cooling (blue) and warming (red) through T_c, and the A$\rightarrow$B (blue) or B$\rightarrow$A (red) transitions are shown in Figure 1. The displacement

of the blue and red arrows in Figure 1 illustrates the hysteresis of the first order A$\rightarrow$B (B$\rightarrow$A) phase transitions. We cooled to within 5 μK of the supercooled transition at 22 bar and maintained the temperature within 5 μK of that transition for a day and observed no A$\rightarrow$B transition, emphasizing the stability of the metastable A phase close to the observed supercooled transition temperature.

The P, T of the A$\rightarrow$B supercooled phase transitions while ramping temperature at ≤ 10 μK/hr is shown in Figure 2(a) as left-pointing triangles with a heavy blue line drawn to guide the eye. These points lie below the equilibrium T_{AB} line (light green)[1] where the free energies of the A and B phases are equal. The light green and blue lines delineate the supercooled A phase (light yellow). The A phase is reliably observed while cooling through T_c below the polycritical point; however, it does not reappear on warming at these pressures, assuring us that the magnetic field is negligible. We observed the A$\rightarrow$B transition at 20.89 bar ~ 24 μK below T_c but no A$\rightarrow$B was seen at 20.88 bar (Supplementary Figure 6). Thus we do not extend the blue line to T_c; instead, we draw a gray dashed line at 20.88 bar. In the supplementary material, we show (Supplementary Figure 3) the set of A$\rightarrow$B transitions observed in the HEC along with the transitions shown here in the IC.

The A$\rightarrow$B transition occurs spontaneously in a narrow

temperature range in "standard" experiments[10], compared to the stochastic Baked-Alaska mechanism. To sample the A→B transition statistics, we overdrove the quartz fork in the IC (by 10×) for a few hundred seconds, to warm the IC above T_c and then cool back through T_c and $T_{A→B}$ as rapidly as possible ($\sim 100\mu$K/hr at $T_{A→B}$). Warming the IC above T_c is essential to prevent premature nucleation by persistent pockets of B phase.

The Q following these pulses is shown in Figure 2(b,c) and also in Supplementary Figure 4. The ^{3}He in the channel is certainly in the A phase before the IC cools through T_c[24, 25, 29, 30] and the ^{3}He in the HEC is in the B phase. In Figure 2(b), the A→B transition occurs in a very narrow interval of Q (and thus T). The width of the distribution of $T_{A→B}$ at 21.4 bar is found to be $\sigma = 3.6$ μK and is shown (in purple) in the inset of Figure 2(a), close to the slow cooled $T_{A→B}$ (dashed purple line), and similarly for 21.1 bar, $\sigma = 3.0$ μK (cyan in inset to Figure 2(a)). At 21.0 bar (green), the fast cooled A→B transitions were more broadly distributed ($\sigma = 6.0$ μK). Pulsed experiments at 20.95 and 20.90 bar showed only a few A→B transitions with most pulsed transitions crossing directly from the normal to the B phase (Supplementary Figure 5). Slow cooled A→B transitions were seen at 20.95, 20.92, 20.90 and 20.89 bar (Supplementary Figure 6). The narrow widths of A→B transitions seen after pulsed heating and their coincidence with slow cooled transitions argue against nucleation by the "Baked Alaska mechanism" (a stochastic process). The scatter in T_{AB} and increase in width of the distribution for fast cooled transitions at low pressures argues for the onset of an instability of the A phase under cooling at constant pressure from T_c.

Resonant tunneling[19] (RT) invokes the presence of an intermediate state between the A and B phases and leads to an enhanced transition probability at specific P,T. Providing the high transition-probability region is transited fast enough to preclude B phase nucleation, another region of A phase stability should be observable. None of the fast cooled transitions resulted in the A phase being stable appreciably below the "blue line" $T_{A→B}$ (P=Const.) in Figure 2(a). Possibly the cooling rate was too slow, or RT is not applicable.

Consequently, we sought to access P,T below the blue line by passing between the lowest constant-pressure $T_{A→B}$ transition and T_c. The dotted purple line in Figure 3 started at 21.6 bar, cooled through T_c, and the pressure was then decreased over $\sim$30 hr to 20.66 bar through the dashed line without observing A→B, cooling to 2.236 mK and then re-pressurizing to 21.21 bar. The last step involved several crossings of the blue line but no A→B transition was observed. On further cooling at constant pressure, we finally observed an A→B transition at 2.221 mK (purple triangle). If the transition observed under constant pressure cooling were due to an enhanced transition probability at (or near) cer-
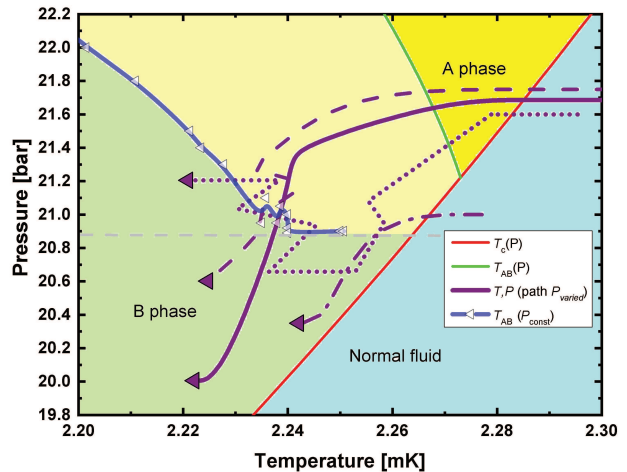

FIG. 3. The path followed (dotted purple line) to search for a supercooled transition related to the RT[19]. Solid, dashed, and dot-dashed purple lines depict paths followed where cooling at constant pressure was followed by depressurization. A→B transitions are denoted by purple triangles.

tain values of (P,T) as predicted by RT, then we should have observed an A→B transition on crossing the $T_{A→B}$ (P=Const.) line. We conclude that P,T are insufficient to describe the state of the system if RT plays a role in the $T_{A→B}$ transition.

The B phase did not nucleate in transit through the dashed grey line. In Figure 3, another path (dot-dashed) started at 21.0 bar and passed through the grey line before a A→B transition occurred at 20.35 bar and 2.242 mK. It thus appears that the supercooled A→B transition (blue line) terminates away from T_c similar to a critical point. (see Supplementary Note 2).

The robustness of the blue line was tested after cooling through T_c and then depressurizing (solid and dashed purple lines in Figure 3). The $T_{A→B}$ (P=Const.) line which appeared to be so well-defined under fast and slow constant-pressure cooling could be crossed readily. Clearly P,T are insufficient to specify the coordinates at which T_{AB} occurs with high probability.

The initiation of the A phase after crossing T_c below the polycritical point (despite the B phase's stability in this P,T) is worth discussion. A small magnetic field would insert an infinitesimal width of A phase between the normal state and the B phase[31]. Our constant-pressure cooled data below the polycritical point bears some resemblance to the data in 0.5 mT of Kleinberg[9] (Supplementary Figure 3). In our experiments, there is no A phase observed below 21.22 bar on warming. Another mechanism to nucleate the A phase below 21.22 bar references Cahn-Hilliard[3] where the surface-energy cost to grow a seed of the B phase in the IC just below T_c from the A phase filled channel (See Supplementary Figure 2) exceeds the volume free-energy cost of the A over
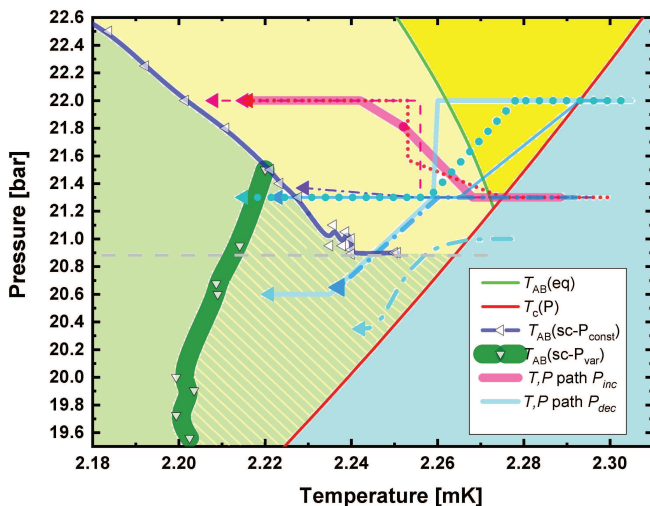
FIG. 4. Cyan lines, with differing symbols show paths from 22 bar to 21.3 bar, from 22 bar to 20.6 bar and from 21.3 bar to 20.6 bar, to observe A→B transitions (blue triangles). A→B transitions were also observed after cooling through T_c at 21.3 bar and then pressurizing to 22 bar (pink and purple lines with differing symbols), terminating in pink and purple triangles. A→B transitions observed following depressurization (or pressurization) retain memory of the pressure that T_c was traversed at since they supercool deeper (or less) than their constant pressure cooled counterparts. Supercooled A→B transitions after depressurizing through the "blue line" below 21.5 bar are shown as downward pointing triangles along a broad green line (guide to the eye).

the B phase. Once the A phase occupies the IC, B phase nucleation requires overcoming a barrier and leads to supercooling. Similarly, once the A phase is established in the IC, passage through the grey line can be understood. However, this cannot explain the persistence of the A phase in P, T below the blue line following the paths in Figure 3.

A→B transitions (paths not shown) were also seen after crossing T_c at various pressures followed by depressurization while slowly cooling. The eventual A→B transition occurred along a scattered line (shown as a broad green line in Figure 4) after passing through the $T_{A→B}$ (P=Const.) line below 21.5 bar. We conclude that depressurization after passage through T_c leads to enhanced supercooling (green/yellow striped region in Figure 4) and a path dependence, effectively registering a memory of the pressure that T_c was crossed at. This raises the question as to why the A→B transition occurs so reproducibly at the P, T coordinates of the "blue line" under constant pressure cooling.

We also compare the supercooling observed by passage through T_c, followed by a pressurization at nearly constant temperature and then cooling at constant pressure to the case of supercooling observed at constant pressure. Indeed *under*-supercooling is seen after pressuriza-

tion, though the extent is not dramatic (pink lines in Figure 4). Similarly, depressurization following cooling at a constant pressure results in *greater* supercooling than a constant pressure cooling through T_c to the same final pressure (Cyan lines in Figure 4). These observations confirm the path dependence of supercooling.

Yip and Leggett introduced the concept of a "lobster pot" (See Fig. 1 in [6]), a ^{3}He filled cavity in a surface connected to the bulk ^{3}He via a narrow orifice. Such a cavity could store a memory of the pressure that T_c is crossed at, but would be unrealistic in size (see Supplementary Note 3); we conclude that "lobster pots" are not the likely source of the path dependence.

It is more likely that domains or even instances of different phases of ^{3}He at surfaces or corners[32] in the IC or from the interface between the channel through which cooling takes place play a role. As we point out in the introduction, there are predictions of novel phases near T_c in bulk[20] and under confinement[21]. Such phases (even in a "virtual state") might allow RT to go forward. But domain walls, formed under specific cooling conditions might play a role[33] and could respond differently under pressurization. It is expected that these free energy landscapes would be sensitive to magnetic fields and boundary conditions[34]. On the other hand classical systems are known to display path dependence in the supercritical region[5] and there may be analogs of these in ^{3}He. The complex $3×3$ matrix order parameter may also play a role in the process of conversion from one phase to another, as the components would have to evolve to effect the transformation.

In conclusion, we have carried out a study of the nucleation of the superfluid B phase of ^{3}He from the supercooled A phase in the vicinity of the polycritical point, where the two phases' free energy difference is small. We find that this supercooled (measured at constant pressure) first order A→B transition occurs reliably along a well defined line of P, T coordinates that terminates at a P, T separated from the second order T_c line. The supercooling is consistent under "fast" (~ 0.1 mK/hr) and "slow" ($\sim$10 μK/hr) cooling except in the vicinity of the terminus point. The supercooling displays a path dependence: P, T alone cannot describe the coordinates where the A phase transforms to the B phase. Supercooling can be enhanced by crossing T_c and then depressurizing. We find that the statistics of the transition are incompatible with the expectations of the Baked-Alaska scenario, and we are unable to confirm or negate the applicability of Resonant Tunneling. While a memory effect can be ascribed to the presence of cavities ("lobster pots"), it is by no means clear that such structures exist in the experimental chamber. Interestingly, the observation that these first order transitions proceed with some degree of reliability (through some as yet not understood path dependent mechanisms) present parallels with evolution in the early universe where the "system" should not evolve

too far out of equilibrium[36]. Thus ^{3}He may well be a useful analog of cosmological evolution.

We are thus left with a new puzzle. The line of constant pressure supercooled transitions is detached from the co-existence line and the A phase nucleates reliably below the polycritical point, perhaps being imprinted because cooling occurs through a superfluid-normal interface with the superfluid stabilized in the A phase because of confinement. The imprinting, if valid, raises the possibility of seeding non-equilibrium phases of ^{3}He by the incorporation of fine periodic and oriented nanoscale structure in a channel[22, 37–39], in a region near the polycritical point where many, nearly equivalent states such as the polar, planar and axi-planar phases of the superfluid may exist[20]. It remains to be explored whether such path dependence is confined to the restricted region near the polycritical point.

---

* Corresponding Author: J.M. Parpia: jmp9@cornell.edu

[1] D. Greywall, ^{3}He melting-curve thermometry at millikelvin temperatures, Phys. Rev. B **31**, 2675 (1985).

[2] D. D. Osheroff and M. C. Cross, Interfacial surface energy between the superfluid phases of ^{3}He, Phys. Rev. Lett. **38**, 905 (1977).

[3] J. W. Cahn and J. E. Hilliard, Free energy of a nonuniform system. i. interfacial free energy, J. Chem. Phys. **28**, 258 (1958).

[4] P. Schiffer and D. D. Osheroff, Nucleation of the AB transition in superfluid ^{3}He: Surface effects and baked alaska, Rev. Mod. Phys. **67**, 491 (1995).

[5] S. Yip and A. J. Leggett, Dynamics of the ^{3}He $A - B$ phase boundary, Phys. Rev. Lett. **57**, 345 (1986).

[6] A. Leggett and S. Yip, Nucleation and growth of ^{3}He $- B$ in the supercooled A-phase, in *Helium Three*, Modern Problems in Condensed Matter Sciences No. 26, edited by L. P.Pitaevskii and W. P. Halperin (Elsevier, Amsterdam, 1990) 3rd ed., Chapt. 8, pp. 523–707.

[7] A. J. Leggett, High-energy low-temperature physics: Production of phase transitions and topological defects by energetic particles in superfluid ^{3}He, J. Low Temp. Phys. **126**, 775 (2002).

[8] G. E. Volovik, *The Universe in a Helium Droplet* (Oxford University Press, 2002).

[9] R. L. Kleinberg, D. N. Paulson, R. A. Webb, and J. C. Wheatley, Supercooling and superheating of the AB transition in superfluid ^{3}He near the polycritical point, J. Low Temp. Phys. **17**, 521 (1974).

[10] P. J. Hakonen, M. Krusius, M. M. Salomaa, and J. T. Simola, Comment on "Nucleation of ^{3}He-B from the A phase: A cosmic-ray effect?", Phys. Rev. Lett. **54**, 245 (1985).

[11] D. S. Buchanan, G. W. Swift, and J. C. Wheatley, Velocity of propagation of the ^{3}He $A - B$ interface in hypercooled ^{3}He $- A$, Phys. Rev. Lett. **57**, 341 (1986).

[12] S. T. P. Boyd and G. W. Swift, New mode of growth of ^{3}He $- B$ in hypercooled ^{3}He $- A$: Evidence of a spin supercurrent, Phys. Rev. Lett. **64**, 894 (1990).

[13] P. Schiffer, M. T. O'Keefe, M. D. Hildreth, H. Fukuyama, and D. D. Osheroff, Strong supercooling and stimulation of the A $-$ B transition in superfluid ^{3}He, Phys. Rev. Lett. **69**, 120 (1992).

[14] C. Bäuerle, Y. M. Bunkov, S. N. Fisher, H. Godfrin, and G. R. Pickett, Laboratory simulation of cosmic string formation in the early universe using superfluid ^{3}He, Nature **382**, 332 (1996).

[15] Y. M. Bunkov and O. D. Timofeevskaya, "Cosmological" scenario for $A - B$ phase transition in superfluid ^{3}He, Phys. Rev. Lett. **80**, 4927 (1998).

[16] T. W. B. Kibble, Topology of cosmic domains and strings, Journal of Physics A: Mathematical and General **9**, 1387 (1976).

[17] W. H. Zurek, Cosmological experiments in superfluid helium?, Nature **317**, 505 (1985).

[18] D. Ki Hong, Q-balls in superfluid ^{3}He, J. Low Temp. Phys. **71**, 483 (1988).

[19] S.-H. H. Tye and D. Wohns, Resonant tunneling in superfluid ^{3}He, Phys. Rev. B **84**, 184518 (2011).

[20] G. Barton and M. A. Moore, Superfluid ^{3}He in restricted geometries, J. of Low Temp. Phy. **21**, 489 (1975).

[21] Y.-H. Li and T.-L. Ho, Superfluid ^{3}He in very confined regular geometries, Phys. Rev. B **38**, 2362 (1988).

[22] J. Pollanen, J. I. A. Li, C. A. Collett, Gannon, W. P. W. J., Halperin, and J. A. Sauls, New chiral phases of superfluid ^{3}He stabilized by anisotropic silica aerogel, Nature Physics **8**, 317 (2012).

[23] V. V. Dmitriev, A. A. Senin, A. A. Soldatov, and A. N. Yudin, Polar Phase of Superfluid ^{3}He in Anisotropic Aerogel, Phys. Rev. Lett. **115**, 165304 (2015).

[24] N. Zhelev, T. Abhilash, E. Smith, R. Bennett, X. Rojas, L. Levitin, J. Saunders, and J. Parpia, The A-B transition in superfluid helium-3 under confinement in a thin slab geometry, Nature Communications **8**, 15963 (2017).

[25] D. Lotnyk, A. Eyal, N. Zhelev, T. Abhilash, E. Smith, M. Terilli, J. Wilson, E. Mueller, D. Einzel, J. Saunders, and J. Parpia, Thermal transport of helium-3 in a strongly confining channel, Nature Communications **11**, 4853 (2020).

[26] L. J. Buchholz, Fermi superfluids at a rough surface, Phys. Rev. B **33**, 1579 (1986).

[27] V. Ambegaokar, P. G. deGennes, and D. Rainer, Landau-ginsburg equations for an anisotropic superfluid, Phys. Rev. A **9**, 2676 (1974).

[28] R. Blaauwgeers, M. Blazkova, M. Človečko, V. B. Eltsov, R. de Graaf, J. Hosio, M. Krusius, D. Schmoranzer, W. Schoepe, L. Skrbek, P. Skyba, R. E. Solntsev, and D. E. Zmeev, Quartz tuning fork: Thermometer, pressure-and viscometer for helium liquids, J. Low Temp. Phys. **146**, 537 (2007).

[29] L. V. Levitin, R. G. Bennett, A. Casey, B. Cowan,

J. Saunders, D. Drung, T. Schurig, and J. M. Parpia, Phase Diagram of the Topological Superfluid ^{3}He Confined in a Nanoscale Slab Geometry, Science **340**, 841 (2013).

[30] A. J. Shook, V. Vadakkumbatt, P. Senarath Yapa, C. Doolin, R. Boyack, P. H. Kim, G. G. Popowich, F. Souris, H. Christani, J. Maciejko, and J. P. Davis, Stabilized pair density wave via nanoscale confinement of superfluid ^{3}He, Phys. Rev. Lett. **124**, 015301 (2020).

[31] D. N. Paulson, H. Kojima, and J. C. Wheatley, Profound effect of a magnetic field on the phase diagram of superfluid ^{3}He, Phys. Rev. Lett. **32**, 1098 (1974).

[32] Y. Tsutsumi, M. Ichioka, and K. Machida, Majorana surface states of superfluid ^{3}He a and b phases in a slab, Phys. Rev. B **83**, 094510 (2011).

[33] I.-S. Yang, S. H. H. Tye, and B. Shlaer, Classical transitions in superfluid helium 3 (2011), arXiv:1110.2045 [cond-mat.other].

[34] P. J. Heikkinen, A. Casey, L. V. Levitin, X. Rojas, A. Vorontsov, P. Sharma, N. Zhelev, J. M. Parpia, and J. Saunders, Fragility of surface states in topological superfluid ^{3}He (2019), arXiv:arXiv:1909.04210 [cond-

mat.supr-con].

[5] P. Schienbein and D. Marx, Investigation concerning the uniqueness of separatrix lines separating liquidlike from gaslike regimes deep in the supercritical phase of water with a focus on widom line concepts, Phys. Rev. E **98**, 022104 (2018).

[36] A. H. Guth, Eternal inflation and its implications, Journal of Physics A: Mathematical and Theoretical **40**, 6811 (2007).

[37] J. J. Wiman and J. A. Sauls, Superfluid phases of ^{3}He in a periodic confined geometry, J. Low Temp. Phys. **175**, 17 (2014).

[38] V. V. Dmitriev, L. A. Melnikovsky, A. A. Senin, A. A. Soldatov, and A. N. Yudin, Anisotropic spin diffusion in liquid ^{3}He confined in nafen, JETP Letters **101**, 808 (2015).

[39] N. Zhelev, M. Reichl, T. S. Abhilash, E. Smith, K. Nguyen, E. Mueller, and J. Parpia, Observation of a new superfluid phase for ^{3}He embedded in nematically ordered aerogel, Nature Communications **7**, 12975 (2016).

SUPPLEMENTARY NOTE 1. PRESSURE DIFFERENCE ACROSS CHANNEL BETWEEN THE IC AND HEC WHILE PRESSURIZING OR DEPRESSURIZING.

We estimate the pressure difference across the channel that must accompany the pressurization or depressurization of the ^{3}He in the system. We start with the equation that links pressure, impedance, viscosity and flow:

$$\Delta P = Z\eta \, dV/dt, \tag{S1}$$

where ΔP [Pa] is the pressure across the channel, Z [m^{-3}] is the impedance, η [kgm^{-1}s^{-1}] is the viscosity of the ^{3}He at T_c, and dV/dt [m^{3}s^{-1}] is the flow rate through the channel accompanying a change in pressure of the system. The impedance for a rectangular channel, $Z = 12 \, l/wd^3$ is defined by its length $l = 100$ μm, width $w = 3$ mm, and height $d = 1.1$ μm, resulting in $Z = 3\times10^{17}$ m^{-3}. The viscosity of the system is largest at T_c and is estimated to be 0.02 [kg m^{-1} s^{-1}][S1]. Our maximum pressurization or depressurization rate was 1.3 bar/day.

To estimate dV/dt we require the molar volume $V_m = 27.36\times10^{-6}$ [m^3 mole^{-1}] and dV_m/dP = -0.185 $\times10^{-6}$ [m^3 mole^{-1} bar $^{-1}$][S2]. The flow rate can be computed by multiplying the molar volume V_m by the molar flow rate, dn/dt

$$dV/dt = V_m \times dn/dt, \tag{S2}$$

and dn/dt can be calculated from the equation

$$dn/dt = -V_{IC}/V_m^2 \times dV_m/dP \times dP/dt. \tag{S3}$$

The volume of the isolated chamber, $V_{IC} = 0.14\times10^{-6}$ [m^3]; we estimate $dV/dt= 1.4\times10^{-14}$ [m^{3}s^{-1}]

Thus, the expected magnitude of the pressure drop across the channel at the maximum pressurization or depressurization rate is 84 Pa or $\sim$ 1 mbar. The impedance of the fill line below mixing chamber temperatures is of order 10^{17} m^{-3}, introducing a pressure drop of the same order as the channel. Above that temperature, the lower viscosity of the ^{3}He implies negligible pressure differences due to pressurization rates. The hydrostatic pressure difference due to the density differences in the liquid (at cryogenic temperatures) and the gas at room temperature is of order 15 mbar, but this is present whether the cell is operated at constant pressure or while being pressurized. In summary, the pressure in the IC while pressurizing or depressurizing is not significantly different from that at the room temperature controller.

SUPPLEMENTARY NOTE 2. ANALOGY OF THE TERMINATION OF THE LINE OF CONSTANT PRESSURE COOLED A→B TRANSITIONS WITH A CLASSICAL CRITICAL POINT.

In Figures 2, 3 and 4 of the main paper (and in the text), we see that the line of constant pressure supercooled A→B transitions terminates away from T_c in analogy with the critical point in classical gas-liquid transitions. However, there are significant differences. Unlike the classical liquid-vapor transition (which is first order but not symmetry breaking), the A→B transition has no volume change and breaks symmetry. While cooling a classical system at constant pressure, supercooling involves conversion from the parent phase below the co-existence line (where the two phases have equal free energies). This supercooled region should be bounded by the coexistence line and a spinodal line defined by the divergence of the isothermal compressibility, or where an extremum point along an isotherm is attained[S3]. The stability of the A phase at temperatures below the line of spinodal-like transitions is puzzling; spinodals designate where the metastable state becomes absolutely unstable. Thus we conclude that the $T_{A \to B}(P=\text{Const.})$ line cannot be a spinodal. However, the stability of the A phase below the $T_{A \to B}(P=\text{Const.})$ line represents a puzzle, because the free energy difference between the two phases is small. It may well be that the tensor and complex nature of the order parameter introduces an additional barrier or rigidity against the conversion from A→B.

It is possible that the extension of the supercooled A phase beyond the two-phase critical point may be related to echoes of the liquid-vapor coexistence line beyond the critical point (the "Widom Line"[S4, S5] connecting fluid heat capacity maxima), but this remains speculative without detailed thermodynamic data. It seems much more likely that the transformation of the complex order parameter from the A to the B phase is the source of the path dependence and the stability of the A phase away from the line of constant pressure cooled A→B transitions.
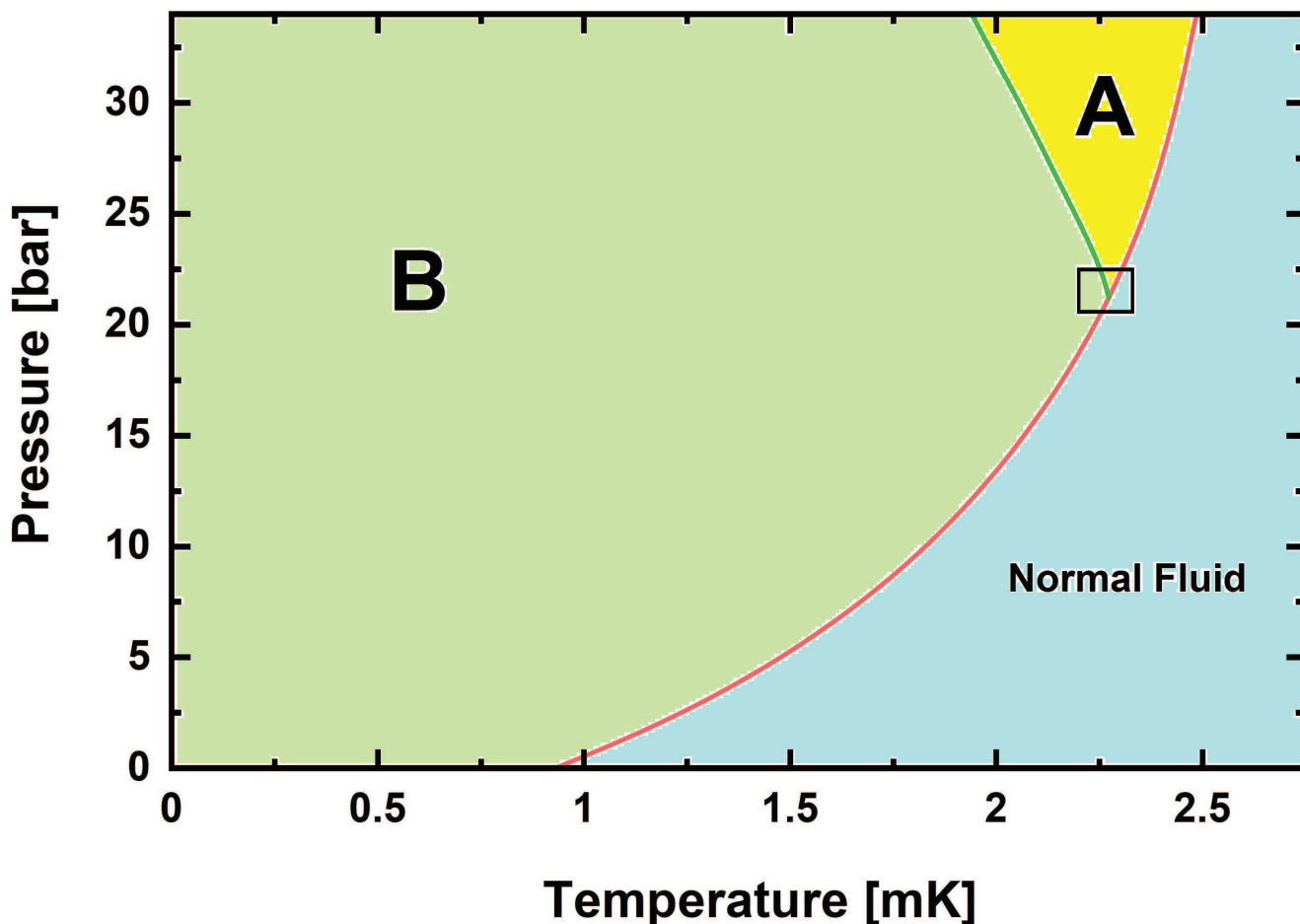
Supplementary Figure S1. The phase diagram of ^{3}He ranging from saturated pressure upto the melting curve. The region investigated in this paper is shown as the box centered on the polycritical point.

SUPPLEMENTARY NOTE 3. LOBSTER POTS.

Yip and Leggett introduced the concept of a "lobster pot" (See Fig. 1 in [S6]), a surface cavity connected to the bulk through an orifice. T_c in the cavity is suppressed relative to the bulk, and T_c in the orifice is further reduced. In this model, the cavity transitions from the normal state to the equilibrium phase at the reduced cavity T_c, encoding the memory of the P, T coordinates of T_c. When the orifice connecting the "lobster pot" to the bulk undergoes T_c, the memory stored in the lobster-pot is imprinted on the bulk. Thus, if the fluid in the IC is cooled through T_c at a high pressure, a "lobster-pot"is filled with A phase. When cooled through T_c near or below the polycritical pressure, the cavity fills with B phase, thus retaining memory of the pressure when it was cooled through T_c. A high pressure cooled experiment should supercool further because an A-phase filled cavity cannot provide a B phase "seed" to nucleate A→B. However, this model requires a very specific distribution of cavities and orifices. For example, to achieve a cavity T_c reduction of 1% requires cavity radii ~ 1 μm[S7, S8], and similar sized pores. Such pore-cavity combinations would favor the A phase even at low pressure, rendering the model problematic.

---

* Corresponding Author: J.M. Parpia: jmp9@cornell.edu

[S1] J. M. Parpia, *The Viscosity of Normal and Superfluid Helium Three*, Ph.D. thesis, Cornell University (1979).

[S2] D. Greywall, ^{3}He specific heat and thermometry at millikelvin temperatures, Physical Review B **33**, 7520 (1986).

[S3] P. G. Debenedetti, Metastable liquids *concepts and principles* (Princeton University Press, Princeton, N.J., 1996) Chap. 2,3, pp. 63–233.
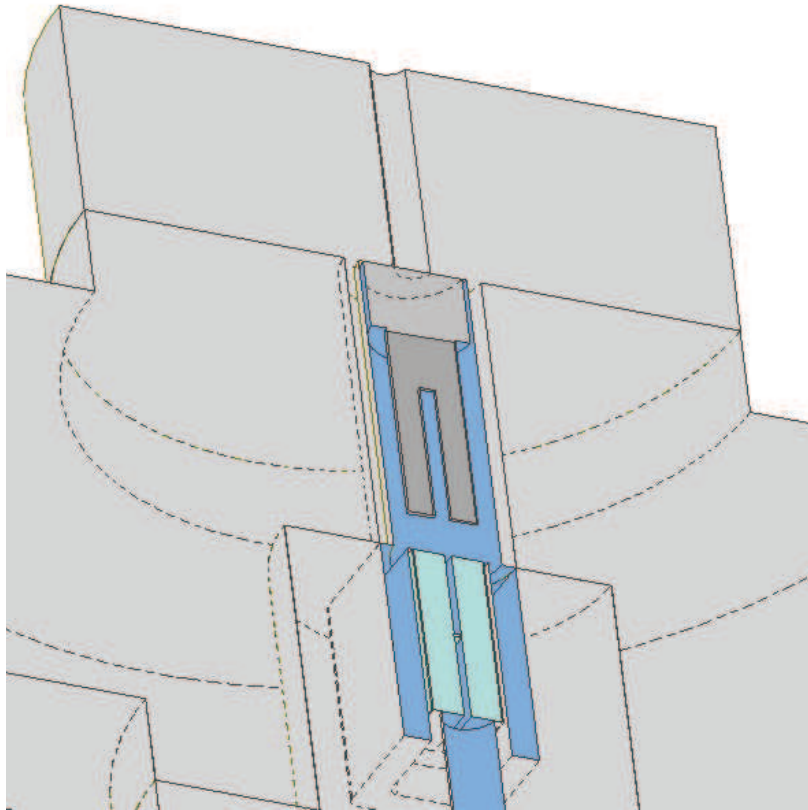
Supplementary Figure S2. Schematic of the IC. The silicon and glass channel is shown as light blue. The open volume (deeper blue) is estimated to be 0.14 cm^3, most of which resides in the bulk liquid surrounding the channel holder and around the quartz fork. There are regions where close fitting coin-silver components that comprise the cell structure are separated by spaced of order 25 μm, that may promote the A phase. All surfaces are as-machined metal.

[S4] L. Xu, P. Kumar, S. V. Buldyrev, S.-H. Chen, P. H. Poole, F. Sciortino, and H. E. Stanley, Relation between the widom line and the dynamic crossover in systems with a liquid–liquid phase transition, Proceedings of the National Academy of Sciences **102**, 16558 (2005), https://www.pnas.org/content/102/46/16558.full.pdf.

[S5] P. Schienbein and D. Marx, Investigation concerning the uniqueness of separatrix lines separating liquidlike from gaslike regimes deep in the supercritical phase of water with a focus on widom line concepts, Phys. Rev. E **98**, 022104 (2018).

[S6] A. Leggett and S. Yip, Nucleation and growth of ^{3}He − B in the supercooled A-phase, in *Helium Three*, Modern Problems in Condensed Matter Sciences No. 26, edited by L. P.Pitaevskii and W. P. Halperin (Elsevier, Amsterdam, 1990) 3rd ed., Chapt. 8, pp. 523–707.

[S7] L. H. Kjäldman, J. Kurkijärvi, and D. Rainer, Suppression of p-wave superfluidity in long, narrow pores, J. Low Temp. Phys. **33**, 577 (1978).

[S8] V. Kotsubo, K. D. Hahn, and J. M. Parpia, Suppression of superfluidity of ^{3}He in cylindrical channels, Phys. Rev. Lett. **58**, 804 (1987).

[S9] R. L. Kleinberg, D. N. Paulson, R. A. Webb, and J. C. Wheatley, Supercooling and superheating of the AB transition in superfluid ^{3}He near the polycritical point, Journal of Low Temperature Physics **17**, 521 (1974).
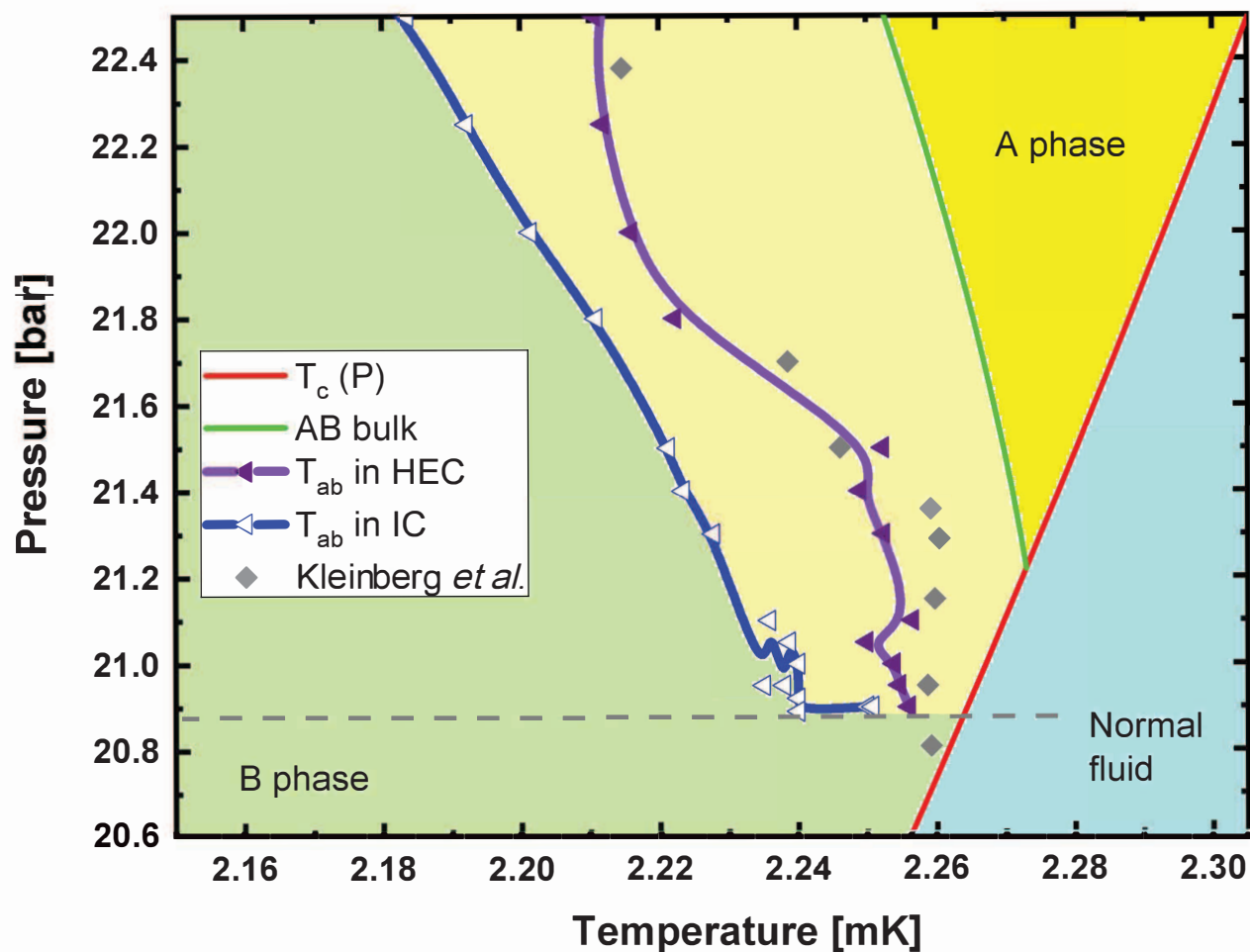
Supplementary Figure S3. The purple left pointing triangles and heavy purple line (guide to the eye) mark the position of the supercooled A→B transitions in the heat exchanger chamber (HEC) compared to the blue, left-pointing triangles and the heavy blue line mark A→B transitions observed in the isolated chamber (IC) show the extent of supercooling of the A phase observed while cooling at constant pressure. The supercooling in the HEC is always observed to be less that that seen in the isolated chamber (IC). The red line shows the location of the second-order phase transition from the normal to the superfluid state $(T_c(P))$ and the cyan line showing the location of the equilibrium A-B transition $(T_{AB}(P))$. Grey diamonds mark the observed transitions shown in the experiments of Kleinberg $etal$.[S9] in a cell where the ^{3}He liquid was in contact with powdered CMN (Cerous Magnesium Nitrate) refrigerant.

5
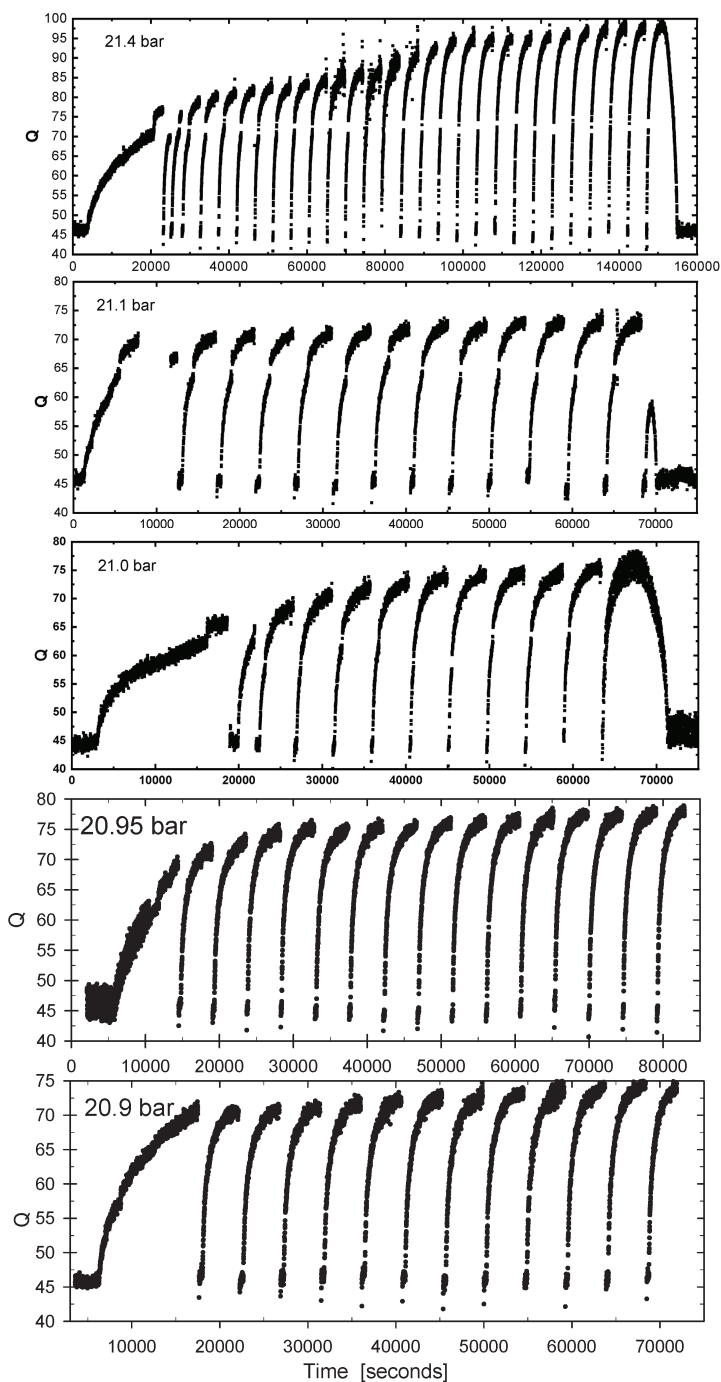
Supplementary Figure S4. Traces of the Q vs time for slow cooled transitions followed by a series of pulses at three different pressures 21.4 bar (top), 21.1 bar, 21.0 bar, 20.95 bar and 21.0 bar (bottom). The A→B transition can be seen as a gap in the Q $vs.t$ traces and is well aligned with the slow cooled transition for the three highest pressures. (See also Fig. 2b, c in the main paper, and Supplementary Figures 5 and 6).
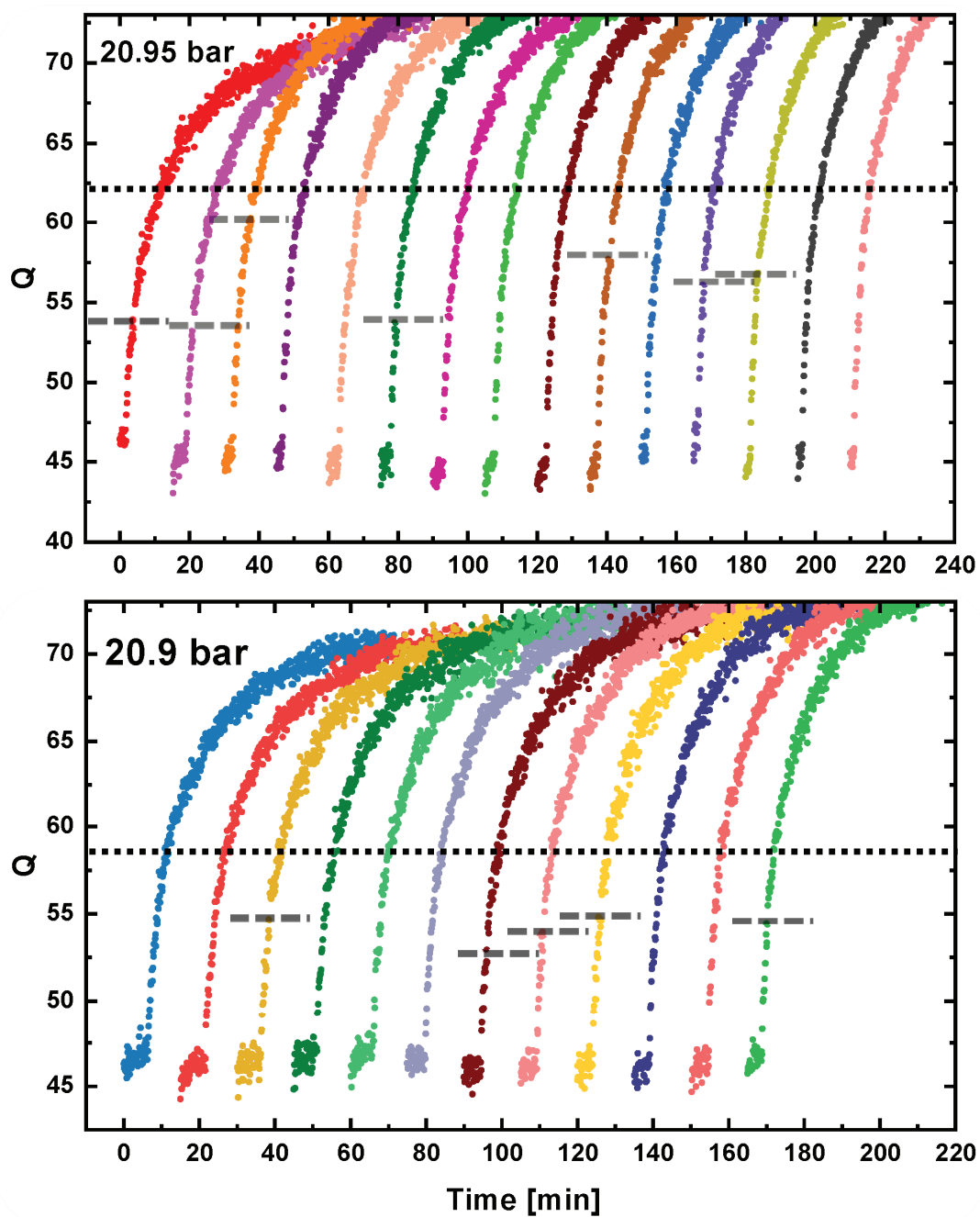
Supplementary Figure S5. Traces of the Q vs time of pulses at the two lowest pressures 20.95 bar (top) and 20.90 bar (bottom) after time shifting. The locations of the slow cooled A→B transition are shown by dotted lines. Poorly defined candidate A→B transitions following pulsed heating are marked by dashed lines. (See also Figure 2 in the main paper, and Supplemental Figures 4 and 6).
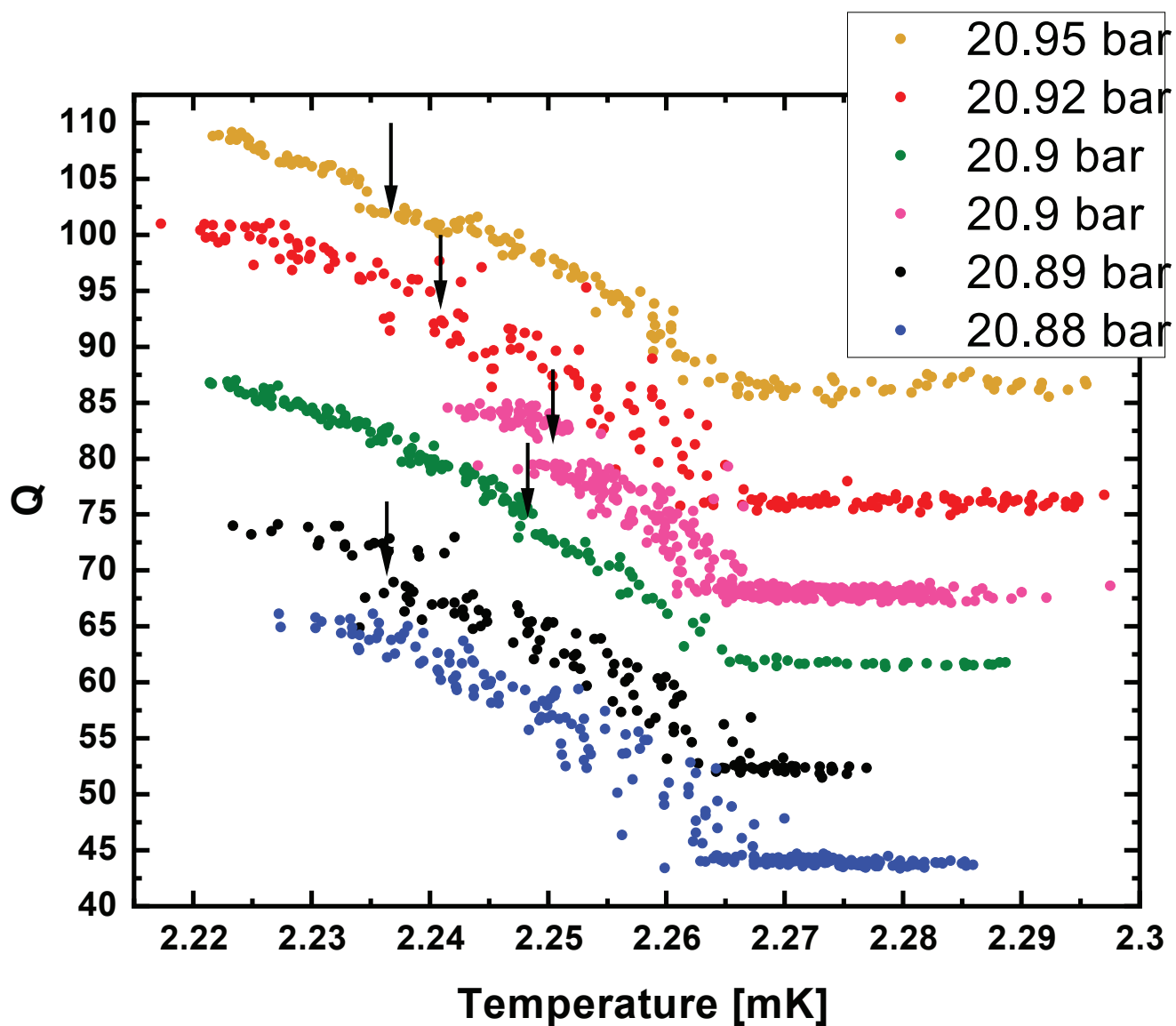
Supplementary Figure S6. Traces of the Q vs temperature for slow cooled transitions at low pressures. The A→B transition is not clearly seen in the pulsed Q $vs.t$ traces though slow cooled transitions show A→B transitions. (See also Fig. 2 in the main paper, and Supplemental Fig. 4). Q values for pressures above 20.88 bar offset by 7 for clarity.